

## Syntheses And Characterization Of Fluorine Doped Tin Oxide Using Spray Pyrolysis Technique.

Agbim, E. G<sup>a</sup>, Ikhioya, I. L<sup>a,b</sup> and Ekpunobi A. J<sup>a</sup>

<sup>a</sup>Department Of Physics And Industrial Physics, Faculty Of Physical Science, Nnamdi Azikiwe University, Awka.

<sup>b</sup>Crystal growth and Material Science Laboratory/Department of Physics and Astronomy, Faculty of Physical Sciences, University of Nigeria, Nsukka, Nigeria  
Corresponding Author: Agbim, E. Ga,

---

**Abstracts:** Fluorine doped tin oxide thin films were successfully deposited onto well cleared glass substrate at different deposition parameters. The XRD patterns of the films showed that the deposited films are polycrystalline in nature having the characteristic peaks of tetragonal structure of SnO<sub>2</sub>. The peaks observed are (110), (101), (200), (211) and the preferential growth along the (110) direction. The current/voltage plots of the material deposited with 10conc.-30conc., which represent sample FT7-FT9 shown a linear plot. It was observed to be Ohmic material. It was also notice that as the dopant concentration of the depositing material increases the thickness of the films increases. The resistivity of the material deposited increases as the dopant concentration and thickness of the films increases. The electrical conductivity of deposited material decreases as the dopant concentration of the material increases. It was observed that as the optical absorbance and reflectance decreases the wavelength of the incident radiation increases and transmittance increases as the wavelength of the incident radiation increases. The films deposited at 10conc.-30conc. recorded energy gap of 2.6eV-3.0eV.

**Keys words:** Spray Pyrolysis, Fluorine, Tin Oxide, XRD and Optical Properties

---

Date of Submission: 30-04-2019

Date of acceptance: 14-05-2019

---

### I. Introduction

Semiconductor thin films have been studied for many years because of their importance in various fields like solar cells and gas sensors [1-5]. Transparent conductive oxides of high band gap semiconductors are mechanically hard and can withstand high temperatures [6-7]. Also wide and direct band gap semiconductor materials are of much interest for blue and ultraviolet (UV) optical devices, such as light-emitting diodes and laser diodes [8]. Semiconductors of SnO<sub>2</sub>:F are known to have a wide range of technological applications, such as transparent conducting electrodes, dye-sensitized solar cells and chemical sensors, and now they seem to be more attractive for their luminescence properties [10]. Tin oxide based thin films are good candidate for a number of applications in many fields of research and in various optoelectronic device fabrications. Most important is the thin film application in environmental monitoring through sensing of a number of gases. Tin oxide characteristics for gas sensing applications have been improved through catalytic and impurity doping with a view of improving on its sensitivity to a number of gases as well as its optoelectronic properties [11-12]. Tin oxide based thin films have been reported to suffer from sensitivity due to the presence of ambient humidity which has been overcome by resistive heating of the thin film gas sensor element [13]. Tin oxide is a wide band gap, non-stoichiometric semiconductor material of n-type conductivity. The conductivity of SnO<sub>2</sub> thin films can be manipulated from normal to degenerate by suitably doping SnO<sub>2</sub> with appropriate amount of halogens [11, 14]. Low electrical resistivity and high visible transmittance are the key elements for solar cell layers, gas sensors, hybrid microelectronics and opto-electronic devices [15]. SnO<sub>2</sub>:F coatings can also act as heat mirrors due to their high reflectivity in the infrared range. Among the various transparent conducting oxides, tin oxide (TO) films doped with fluorine or antimony are most promising due to their chemical inertness and mechanical hardness along with low electrical resistivity and good optical transmittance. Tin oxide is the first transparent conductor to have received significant commercialization [16]. The application of thin films in modern technology is widespread. The methods employed for thin-film deposition can be divided into two groups based on the nature of the deposition process viz., physical or chemical. The physical methods include physical vapour deposition (PVD), laser ablation, molecular beam epitaxy, and sputtering. The chemical methods comprise gas-phase deposition methods and solution techniques. The gas-phase methods are chemical vapour deposition (CVD) and atomic layer epitaxy (ALE), while spray pyrolysis, sol-gel, spin and dip-coating methods employ precursor solutions [17]. Among the various deposition techniques, the spray pyrolysis is well suited for the

preparation of doped tin oxide thin films because of its simple and inexpensive experimental arrangement, ease of adding various doping material, reproducibility, high growth rate, and mass production capability [16]. Spray pyrolysis is a processing technique being considered in research to prepare thin and thick films, ceramic coatings, and powders. Unlike many other film deposition techniques, spray pyrolysis represents a very simple and relatively cost-effective processing method (especially with regard to equipment costs). It offers an extremely easy technique for preparing films of any composition. It does not require high-quality substrates or chemicals. The method has been employed for the deposition of dense films, porous films, and for powder production. Even multi layered films can be easily prepared using this versatile technique. Spray pyrolysis has been used for several decades in the glass industry and in solar cell production [17]. Typical spray pyrolysis equipment consists of an atomizer, precursor solution, substrate heater, and temperature controller. The following atomizers are usually used in spray pyrolysis technique: air blast (the liquid is exposed to a stream of air) [18], ultrasonic (ultrasonic frequencies produce the short wavelengths necessary for fine atomization) and electrostatic (the liquid is exposed to a high electric field) [19].

## II. Experimental Details

### 2.1 Materials And Methods

The various materials were used in the fabrication of the films; Glass substrate, Spray pyrolysis machine, Ethanol and water as solvent, Precursor  $\text{SnCl}_4$  (MERCK), Dopant Ammonium fluoride (BDH), Four-point probe, X-ray diffractometer and UV visible spectrophotometer. Spray pyrolysis technique was used for this deposition. It involves spraying of a solution containing soluble salts of the desired compound onto heated substrates, where the constituents react to form a chemical compound. The chemical reactants used for making solution are selected such that the products other than the desired compound are volatile at the temperature of deposition. Every sprayed droplet reaching the surface of the hot substrate undergoes pyrolytic decomposition and forms a single crystalline or cluster of crystallites as a product. The other volatile by-products and solvents escape in the vapour phase. The substrates provide thermal energy for the thermal decomposition and subsequent recombination of the constituent species.

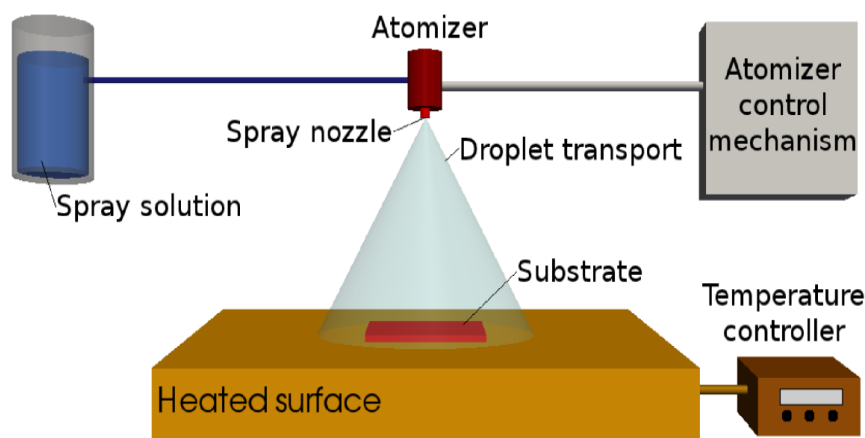


**Figure 1:** General schematic of a spray pyrolysis deposition process.

### 2.2 Substrate (Microscopic Glass Substrate)

The substrate used here is a microscopic glass substrate. Hand gloves were used to handle the substrates to avoid contamination. The substrates were dipped in acetone, methanol, rinsed with distilled water and later ultra-sonicated for 30 min in acetone solution after which they were rinsed in distilled water and kept in an oven at 333K to dry.

### 2.3 Spray Process/Procedure

The spray process involves optimization of several process parameters. The values of the optimized process parameters are: Precursor flow rate 0.07ml/min, Solvent 90% ethanol, Precursor ( $\text{SnCl}_4$ ) concentration 0.1mol, Dopant Ammonium Fluoride, Dopant concentration (0.1mol), Spray-nozzle specification: outside diameter: 0.34mm. Internal diameter 0.18mm, Spray nozzle to substrate distance: 8mm, Substrate temperature 400°C and Atomizing voltage 4.0KV

### 2.4 Experimental Procedure

Thin films of fluorine doped tin oxide were deposited on a transparent glass substrate using  $\text{SnCl}_4$  dissolved in 90ml of ethanol and 10ml of water. The  $\text{SnCl}_4$  was used as source of Sn while  $\text{NH}_4\text{F}$  as the

source of doping impurities. During the deposition, the films were deposited at a constant temperature and voltage rate of 400°C and 3.8KV respectively. The substrate was attached to the substrate holder, with the temperature regulator; the substrate was heated to the temperature of 400°C. The voltage was set to 3.8KV via the voltage knob and the precursor solution of SnCl<sub>4</sub> and NH<sub>4</sub>F was passed through the nozzle pump direct to the nozzle. As the mixture gets to the substrate through the nozzle and hits the surface of the substrate, evaporation of the residual solvent takes place, spreading of the droplet and then the salt decomposition SnO<sub>2</sub>:F was finally deposited on the substrate. Film uniformity was ensured by moving both the nozzle (needle) and the substrate. Different levels of doping were achieved by varying the amount of NH<sub>4</sub>F in the precursor solution from 0.1 to 0.3M. The films with different level of doping were deposited on the glass substrate at temperature of 400°C. Uniformity of temperature over the entire substrate and fine sprays were necessary to obtain good quality films which are reproducible. The temperature during spray was 400°C with the help of the temperature controller whereas the dopant concentration of NH<sub>4</sub>F was varies (see table 1). After spraying, the substrates were allowed to be cooled at room temperature.

**Table 1:** Variations of dopant concentration parameters for fabrication.

Samples	Dopant NH <sub>4</sub> F (%)	SnCl <sub>4</sub> (ml)	Ethanol (ml)	Voltages (KV)	Temperature (Degree)
FT7	10	20	5	3.8	400
FT8	20	20	5	3.8	400
FT9	30	20	5	3.8	400

### 2.5 Characterization Of Fabricated Films.

The fabricated films were characterized using three different instruments for the analysis. The optical analysis were carried out using MT670 UV- visible spectrophotometer where the absorbance of each of the samples was obtain and other optical properties were obtained by calculation. Electrical (I/V) characterization of thin films was done using the four-point probe method at room temperature. The measurements were taken in a square geometry using Keithley2400 Source Meter. This was carried out at Sheda Science and Technology Complex, Abuja. The structural characterization of the films was carried out using cu-kal ( $\lambda = 1.5418\text{\AA}$ ) DD-15.5 standard diffractometer, the instrument helped in determining the type of crystal lattice and intensities of diffraction peaks, with the help of data base software supplied by the international center of diffraction data. The characterization was carried out at IThemba LABS Materials Research Department South Africa.

## III. Results And Discussion

### 3.1 Structural Analysis

The XRD analysis was carried out to determine the phase angel, crystallite size and dislocation density of the films deposited by varing the dopant concentration of the films., deposition voltage, temperature were kept constant. The XRD patterns of the films prepared by different deposition parameters showed that the deposited films are polycrystalline in nature having the characteristic peak of tetragonal crystal structure. The peaks observed are (110), (101), (200), (211) (see table 2) and among all the peaks the orientation of (110) peak is the highest intensity peak. This is observed in the patterns of all the films with different deposition parameters of SnO<sub>2</sub>:F films prepared from SnCl<sub>4</sub> precursor, which also revealed the preferential growth along the (110) direction. The crystallite sizes of the deposited SnO<sub>2</sub>:F films were determined from Scherer's equation (1) [20].

$$D = \frac{0.94\lambda}{\beta \cos\theta} \quad (1)$$

where D is the crystallite size in nanometers,  $\beta$  is the full width at half maximum of the diffraction line measured in radians and  $\lambda$  is the wavelength of X-ray used ( $\lambda = 1.5418\text{\AA}$ ). The dislocation density  $\delta$  is calculated using equation 2[21-22]. See Figure 2 for the XRD pattern

$$\delta = \frac{1}{D^2} \text{ lines/m}^2 \quad (2)$$

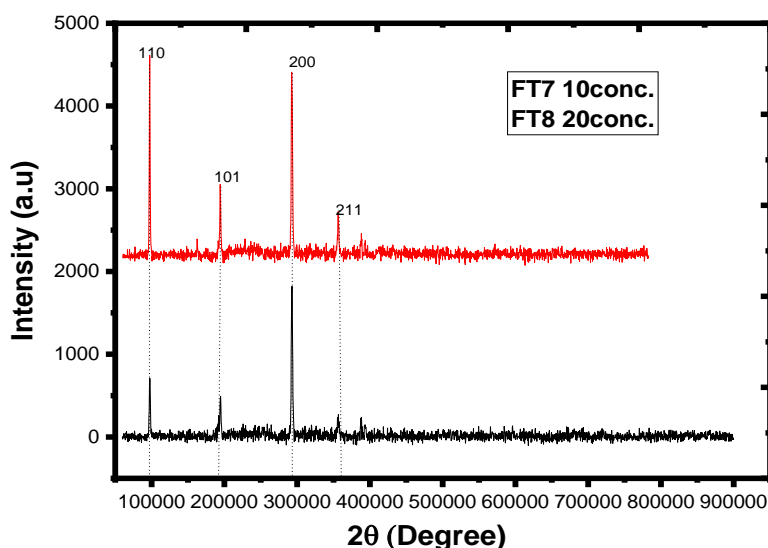


Figure 2: XRD pattern of SnO<sub>2</sub>:F

Table 2: Structural parameters

Sample/ Thickness	2θ (degree)	D (spacing)Å	(β) FWHM	(hkl)	Lattice(a) Å	Grain Size(D)nm	Dislocation density (δ) x10 <sup>12</sup> lines/m <sup>2</sup>
FT7/ 192.609nm	10.3256	3.294	0.0291	110	4.7309	50.0067	3.9989
	20.2987	3.285	0.0291	101		50.5956	3.9064
	30.1943	3.265	0.0291	200		51.5843	3.5515
	37.2872	3.243	0.0291	211		52.5620	3.6100
FT8/ 199.502nm	10.3256	3.299	0.0291	110		50.0087	3.9986
	20.2987	3.280	0.0291	101		50.5816	3.9085
	30.1943	3.262	0.0291	200		51.5931	3.7525
	37.2872	3.244	0.0291	211		52.2396	3.6644

### 3.2 Electrical Analysis

Electrical characterization of thin films was done using the four-point probe method at room temperature. The measurements were taken in a square geometry using Keithley2400 Source Meter. From (fig. 3 and table 3) the current versus voltage plots of the material deposited with 10conc.-30conc., which represent sample FT7-FT9 shown a linear plot. It was observed to be Ohmic material. It was also notice that as the dopant concentration of the depositing material increases the thickness of the films increases. The resistivity of the material deposited increases as the dopant concentration and thickness of the films increases. The electrical conductivity of deposited material decreases as the dopant concentration of the material increases [23-24].

Table 3: Calculated values of resistivity and conductivity

Samples	Thickness, t (nm)	Resistivity, ρ (Ωm)	Conductivity, σ (Ωm) <sup>-1</sup>
FT7(10conc.)	192.609	6.6730x10 <sup>4</sup>	1.4985x10 <sup>-5</sup>
FT8(20conc.)	199.502	7.6030x10 <sup>5</sup>	1.3155x10 <sup>-6</sup>
FT9(30conc.)	205.105	8.3400x10 <sup>7</sup>	1.1990x10 <sup>-8</sup>

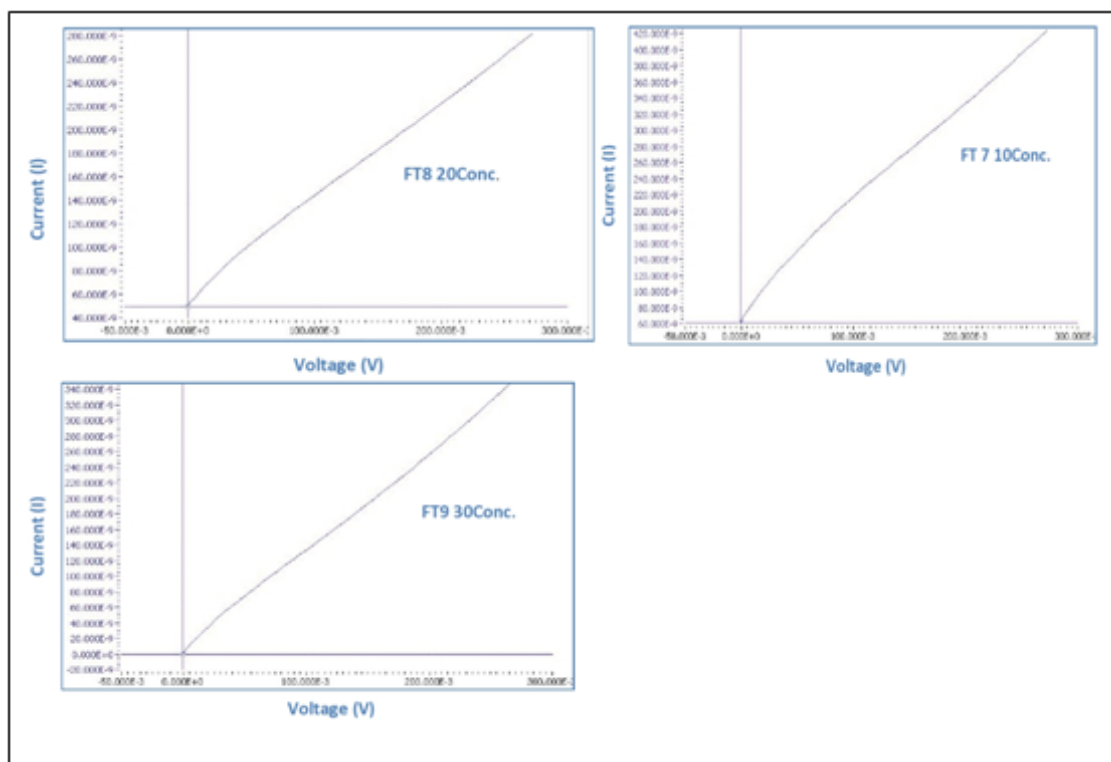


**Figure 3:** Current versus Voltage plot of sample FT7-FT9

### 3.3 Optical Properties

Optical characterization of the thin films was done using the UV-visible spectrophotometer from (fig.5) it was observed that as the optical absorbance decreases the wavelength of the incident radiation increases. It was noticed that sample FT8 deposited at 20conc. emerged the highest absorbance with absorbance value of 0.592 at incident wavelength of 340nm followed by sample FT7 deposited at 10conc. with absorbance value of 0.543 at incident wavelength of 320nm. Hence, it is very clear that sample FT9 deposited at 30conc. emerged the lowest with absorbance value of 0.532 at incident wavelength of 320nm. Therefore, the optical absorbance of the deposited material decreases as the dopant concentration of the deposited material ( $\text{SnO}_4:\text{F}$ ) increases with the wavelength of the incident radiation [11]. From (fig.6) it was observed that as the optical transmittance increases as the wavelength of the incident radiation increases. It was noticed that sample FT9 deposited at 30conc. emerged the highest transmittance with transmittance value of 0.778 at incident wavelength of 1490nm followed by sample FT8 deposited at 20conc. with transmittance value of 0.773 at incident wavelength of 1480nm followed by sample FT7 deposited at 10conc. with transmittance value of 0.756 at incident wavelength of 700nm. Therefore, the optical transmittance of the deposited material increases as the dopant concentration of the deposited material ( $\text{SnO}_4:\text{F}$ ) increases with the wavelength of the incident radiation [25]. From (fig.7). It was noticed that sample FT7 deposited at 10conc. emerged the highest reflectance with reflectance value of 0.20349 at incident wavelength of 1480nm followed by both sample FT8 deposited at 20conc. and sample FT9 deposited at 30conc. with reflectance value of 0.20346 at incident wavelength of 440nm. Hence, the optical reflectance of the deposited material decreases as the dopant concentration of the deposited material ( $\text{SnO}_4:\text{F}$ ) increases with the wavelength of the incident radiation [25].

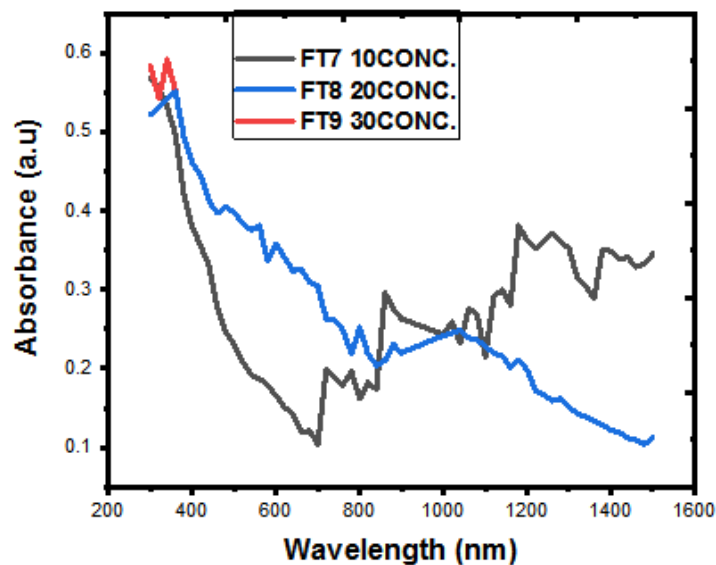


**Figure 4:** The optical absorbance versus wavelength

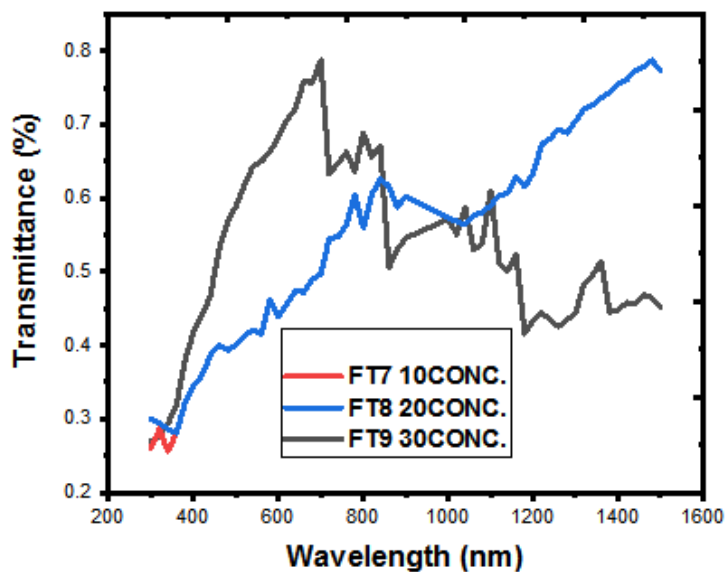


**Figure 5:** The optical transmittance versus wavelength

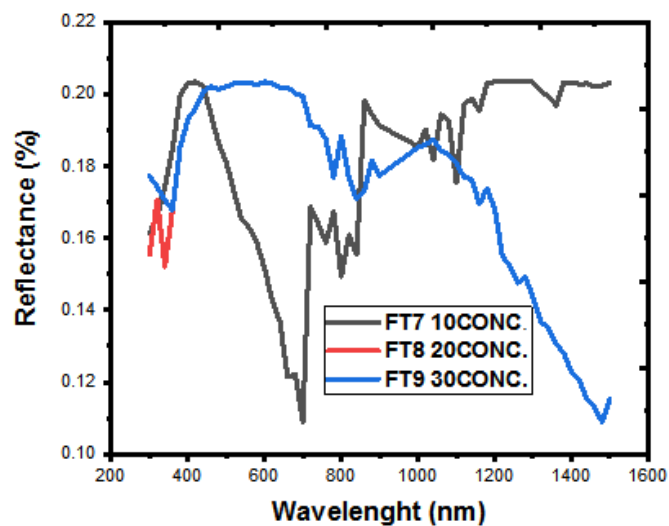


**Figure 6:** The optical reflectance versus wavelength

The band gap energy of the deposited material was obtained using

$$\alpha h\nu = A(h\nu - E_g)^n$$

Where  $A$  is a constant,  $E_g$  is the energy band gap of the material deposited (F: SnO<sub>4</sub>),  $h$  is the plank constant and  $n = \frac{1}{2}$  for direct allowed transition. This relation establishes that a plot of  $(\alpha h\nu)^2$  versus  $h\nu$  produces a linear pattern the intercept on  $h\nu$  axis being the energy band gap,  $E_g$  of the thin film. The plot is not direct [26]. The extrapolations of the direct portions of plots to the energy axis give the band gap energy. From (fig.7) which represents the material deposited at 10conc.-30conc. Recorded energy band gap of 2.5eV-3.0eV.

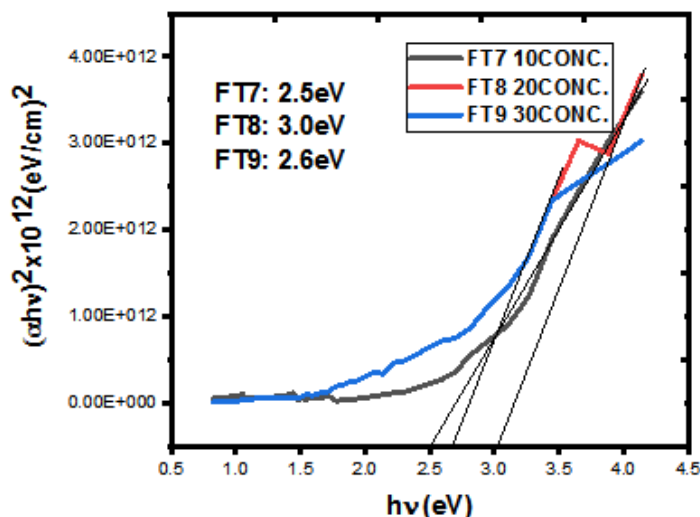


**Figure 7:** The absorption coefficient square versus photon energy FT7

From (Fig. 8), It was noticed that sample FT7 deposited at 10conc. emerged the highest refractive index with refractive index value of 2.6406, sample FT8 deposited at 20conc with refractive index value of 2.6397 followed by sample FT9 deposited at 30conc. with refractive index value of 2.6047. Therefore, the optical refractive index of the deposited material increases as the dopant concentration of the deposited material (SnO<sub>4</sub>:F) increases with the photon energy [11]. From (fig. 9) it was observed that the extinction coefficient increases as the photon energy increases. It was noticed that sample FT8 deposited at 20conc. recorded the highest extinction value of 0.04710, sample FT7 deposited at 10conc. with extinction coefficient value of 0.04527 follow by sample FT9 deposited at 30conc. with extinction coefficient value of 0.041531. Hence, the extinction coefficient of the deposited material increases and then increased as the dopant concentration of the deposited material (SnO<sub>4</sub>:F) increases with the photon energy [27]. From (Fig.10) shows that as the optical conductivity increases with the photon energy. It was noticed that sample FT7 deposited at 10conc. and sample FT8 deposited at 20conc. emerge the highest with optical conductivity value of 1.06938E+14 follow by sample FT9 deposited at 30conc. with optical conductivity value of 1.01979E+14. Hence, the optical conductivity of the deposited material decreases as the dopant concentration of the deposited material (SnO<sub>4</sub>:F) increases with the photon energy [11].

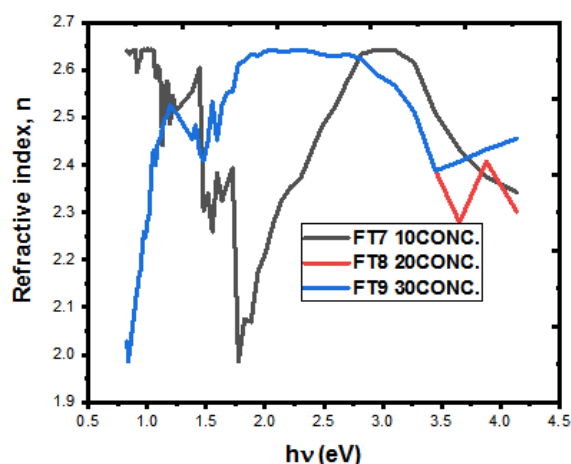


**Figure 8:** The refractive index versus photon energy

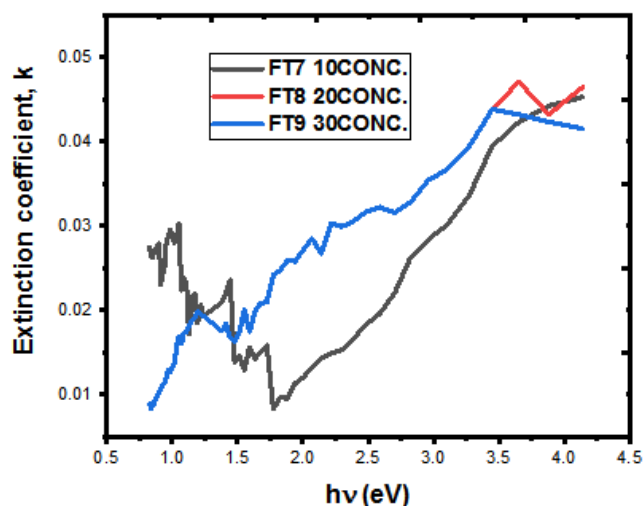


Figure 9: The extinction coefficient versus photon energy

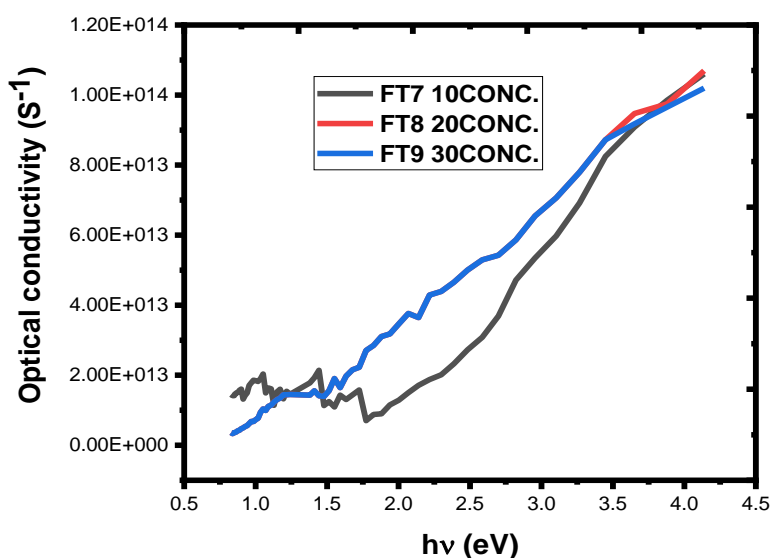


Figure 10: The optical conductivity versus photon energy

#### IV. Conclusion

Fluorine doped tin oxide thin films have been successfully deposited and characterized at different deposition parameters. The absorbance, reflectance decreases and transmittance of the films increases as the wavelength of the films increases with incident radiation. It was observed that as the voltage of the films increases the thickness of the films increases. The conductivity of the films was observed to be increasing with decrease in voltage.

#### Acknowledgement

The authors are grateful to the staff of iThemba Laboratory of Materials Research Department South Africa, the staff of energy centre, ABU-Zaria, and finally Kaduna Polytechnic Centre for Minerals Research & Development Science and Technology Education Post-basic (Step-B) Project (World Bank Assisted) were the characterization was done.

#### References

- [1]. Shanthi S., Subramanian C., and Ramasamy P. (1999). Growth and characterization of antimony doped tin oxide thin films. *Journal of Crystal Growth* 197, 858-864.
- [2]. Ikhioya I. Lucky. Optical and electrical properties of copper telluride thin films. *International Journal of Research in Chemistry and Environment*. 2015;5(3):28-32
- [3]. Ikhioya I. Lucky, Ehika, Simon, Ijabor B. Okeoghene. Influence of deposition potential on lead sulphide (PbS) thin film using electrodeposition technique. *Asian Journal of Chemical Sciences*. 2018;3(4):1-8. DOI: 10.9734/AJOCS/2017/40415



- [4]. Ehika S, Ikhioya I. Lucky. Effects of solution concentration of the optical and electrical properties of lead sulphide (PbS) semiconductor thin films deposited by electrodeposition technique. *Nigerian Annals of Natural Sciences*. 2017;16(1):066–075.
- [5]. Ehika S, Ikhioya I. Lucky. Electrodeposition and characterization on the electrical and optical properties of lead sulphide (PbS) thin films semiconductor. *Nigerian Annals of Natural Sciences*. 2017;16(1):057–065
- [6]. Udofia KI, Ikhioya I. Lucky. Electrical properties of electrodeposited lead selenide (PbSe) thin films. *Asian Journal of Physical and Chemical Sciences*. 2018;5(4):1-7. DOI: 10.9734/AJOPACS/2018/40383
- [7]. Ikhioya I. Lucky, P. O. Orji, Osolobri B. U., Ijabor, B. O and P. N. Okanigbuan Investigation of the Optical and Electrical Properties of Copper Telluride and Cadmium Telluride Thin Films Using Electrodeposition Technique. 2018; 19(1): 1-9. DOI: 10.9734/PSIJ/2018/43238
- [8]. Ikhioya I. Lucky, S. Ehika and N. N. Omehe. Electrochemical Deposition of Lead Sulphide (PbS) Thin Films Deposited on Zinc Plate Substrate. 2018; 1(3): 1-11. DOI: 10.9734/JMSRR/2018/44355
- [9]. Ikhioya I. Lucky. Characterization of Zinc Sulphide Thin Film Prepared by Electrodeposition Method. *International Journal of ChemTech Research* 2015; 8(2): 655-660
- [10]. Babar A. R., Shinde. S., Moholkar A.V., Bhosale C. H., Kim J. H and Rajpure K. Y. (2011). Physical properties of sprayed antimony doped tin oxide thin films: the role of thickness. *Journal of Semiconductors* 32 (5) 1-8.
- [11]. Patrick M. M., Musembi R., Munji M., Odari B., Munguti L., Ntilakigwa A. A., Nguu J., Aduda B. and Muthoka B. (2015). Effects of annealing and surface passivation on doped SnO<sub>2</sub> thin films prepared by spray pyrolysis technique. *Advances in materials* 4 (3) 51-58.
- [12]. [12a] Mwathe P.M., Musembi R., Munji M., Odari B., Munguti L., Ntilakigwa A. A., Nguu J., Aduda B. and Muthoka B. (2014a). Surface passivation effect on CO<sub>2</sub> sensitivity of spray pyrolysis deposited Pd-F: SnO<sub>2</sub> thin film gas sensor. *Advances in materials*. 3 (5) 38-44.  
[12b] Mwathe P.M., Musembi R., Munji M., Odari B., Munguti L., Ntilakigwa A. A., Nguu J., Aduda B. and Muthoka B. (2014b). Influence of surface passivation on optical properties of spray pyrolysis deposited Pd-F:SnO<sub>2</sub>. *International journal of materials science and applications*. 3 (5) 137-142.
- [13]. Odari B.M., Musembi R.J., Mageto M. J., Othieno H., Gaiho F., Mghendi M. and Muramba (2013). **Optoelectronic Properties of F-co-doped PTO Thin Films Deposited by Spray Pyrolysis.** *American Journal of Materials Science* 3(4), 91-99
- [14]. Subramanian N.S, Santhi B, Sundareswaran S. and Venkatakrishnan K.S. (2006). Studies on Spray Deposited SnO<sub>2</sub>, Pd:SnO<sub>2</sub> and SnO<sub>2</sub> :F Thin Films for Gas Sensor Applications. Synthesis and Reactivity in Inorganic. *Metal-Organic and Nano-Metal Chemistry*, 36, 131-135.
- [15]. Ravichandran k., Muruganatham G., Sakthivel B., and Philominathan P. (2009). Nanocrystalline doubly doped tin oxide films deposited using a simplified and low-cost spray technique for solar cell applications. *Journal of ovonic research*, 5 (3) 63-69.
- [16]. Demet T., Güven T. and Bahattin D. (2011). Effect of substrate temperature on the crystal growth orientation and some physical properties of SnO<sub>2</sub>: F thin Films deposited by spray pyrolysis technique. *Rom. Journal Phys.*, 58, 1–2, 143–158.
- [17]. Dainius P and Ludwig J. G. (2005). Thin Film Deposition Using Spray Pyrolysis. *Journal of Electroceramics*, 14, 103–111.
- [18]. Balkenende A.R., Bogaerts A., Scholtz J.J., Tjiburg R.M., and Willems H. (1996). Thin film deposition using spray pyrolysis. *Philips Journal of Research*, 50 (3), 365-373.
- [19]. Jaworek A., Sobczyk A. T., Krupa A., Lackowski M. and Czech T. (2009). Electrostatic deposition of nano thin films on metal substrates. *Journal of Technical Sciences* 57 (1) 63-70
- [20]. Kandasamy P. and Lourdasamy A. (2014). Studies on zinc oxide thin films by chemical spray pyrolysis technique. *International journal of physics*, 9 (11) 261-266.
- [21]. Yadav A.A., Masumdar E.U., Moholkar A.V., Neumann-Spallart M., Rajpure K.Y and Bhosale C.H. (2009). Electrical, structural and optical properties of SnO<sub>2</sub>: F thin films: Effect of the substrate temperature. *J. Alloys Compd.*, 488: 350-355
- [22]. Noh S.I., Ahn H.J. and Riu D.H. (2012). Photovoltaic property dependence of dye-sensitized solar cells on sheet resistance of FTO substrate deposited via spray pyrolysis. *Ceramics Int.*, 38: 3735-3739.
- [23]. Chantarat N., Yu-Wei C., Shu-Han H., Chin-Ching L., Mei-Ching C. and San-Yuan C. (2013). Effect of oxygen on the microstructural growth and physical properties of transparent conducting fluorine-doped tin oxide thin films fabricated by the spray pyrolysis method. *ECS journal of solid state science and technology*, 2 (9) 131-135.
- [24]. Arle R. N and Khatik B. L. (2014). Effect of volume spray rate on highly conducting spray deposited fluorine doped SnO<sub>2</sub> thin films. *International journal of chemical and physical sciences* (3) 83-88.
- [25]. Kim K.S., Yoon S.Y., Lee W.J and Kim K.H. (2001). Surface morphologies and electrical properties of antimony-doped tin oxide films deposited by plasma enhanced chemical vapour deposition. *Surface and coatings technology*, 138 (2), 229-236.
- [26]. Harbeke, G. (1972). Optical properties of semiconductors; in optical properties of solid, *North-holland Pub. Co Amsterdam* 255-272.
- [27]. Sharma A., Prakah D. and Verma K.D. (2007). Post annealing effect on SnO<sub>2</sub> thin films grown by thermal evaporation technique. *Optoelectronics and advanced materials – Rapid communications*, 1 (12), 683-688.

IOSR Journal of Applied Physics (IOSR-JAP) is UGC approved Journal with Sl. No. 5010, Journal no. 49054.

Agbim, E. Ga " Syntheses And Characterization Of Fluorine Doped Tin Oxide Using Spray Pyrolysis Technique." IOSR Journal of Applied Physics (IOSR-JAP) , vol. 11, no. 3, 2019, pp. 70-78.

